

Chapter e14

Projections and Reformations

14.1 INTRODUCTION

In 2002, the American Heart Association proposed a standardized segmentation and accompanying 2D Bull's Eye Plot of the myocardium, or heart muscle, of the left heart ventricle [Cerqueira et al., 2002a]. Figure e14.1 shows how the Bull's Eye Plot (BEP) is constructed by projecting segments of the myocardium onto the horizontal plane, almost as if folding open the heart. Based on this standardized segmentation, information from 3D scans, such as for example the presence of scar tissue, can also be projected onto the Bull's Eye Plot and presented in a clear and unambiguous fashion. The cardiac BEP is a simple but excellent example of *reducing* complex 3D data to a standardized 2D representation that greatly facilitates the interpretation and communication of that data.

In medical visualization, there are a number of similar techniques that are employed to reduce 3D data, either by projection or reformation, to effective 2D visual representations. Straightforward projection, as employed in the standard 3D graphics pipeline, also serves to reduce 3D data to a 2D representation. However, in this chapter we discuss examples that go a step further in terms of complexity and effectiveness.

We have classified these reductive techniques broadly into two groups: *projections* and *reformations*. In projections, 3D information is accumulated, or flattened, along one or more directions to obtain a 2D image. In reformations, 3D information is sampled along some geometry that can later be flattened, and the sampled information along with it. There are examples that have characteristics of more than one class. The Bull's Eye Plot mentioned above is an example of a projection (data is aggregated through the heart wall) with elements of reformation (reformatting to the plane is performed along the geometry of the heart wall), whereas multiplanar reformatting (MPR), or slicing through volumetric data, is clearly a straightforward example of reformation.

14.2 OVERVIEW

We have further grouped the techniques into different types based on their core principles. In this section, we briefly define the different types. In the subsequent sections, we discuss each of the examples in more depth. The types are defined as follows:

- *Anatomical unfolding* techniques rely on a surface describing some anatomical, usually wrinkled, shape in detail, and then unfold that surface, along with the information it holds, onto the view plane. examples motivated by the great deal of self-occlusion that occurs when viewing these complex surfaces. The geometry is fully determined by the anatomy, in contrast to anatomical planar reformation, where the geometry is only partly determined by the anatomy, usually by some sort of center line.
- With *Anatomical planar reformation/projection* techniques, an *anatomically-guided* planar geometry is derived along which samples from the original data can be interpolated and/or aggregated. The planar geometry is then flattened, taking the sampled data along with it.

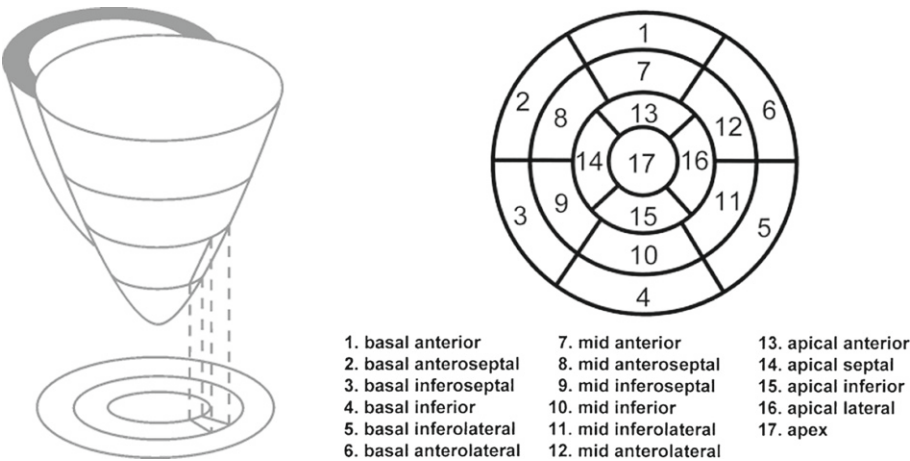


FIGURE e14.1 The cardiac Bull's Eye Plot. **Left:** Principle of construction (courtesy of Steffen Oeltze, University of Magdeburg). **Right:** The resulting myocardial (heart muscle) segments (Courtesy of Konrad Mühler, inspired by [Cerqueira et al. \[2002a\]](#)).

Name	Reference	Type
Cardiac/Volumetric Bull's Eye Plot	Cerqueira et al. [2002a] , Termeer et al. [2007]	AU
Colon Unfolding	Vilanova et al. [2001]	AU
Brain Flattening	Fischl et al. [1999]	AU
Curved Planar Reformation	Kanitsar et al. [2002]	APR/P
Articulated Planar Reformation	Kok et al. [2010]	APR/P
Tubular Straightening	Angelelli and Hauser [2011]	APR/P
Tumor Maps	Rieder et al. [2010]	MP
Liver Resection Surface Maps	Lamata et al. [2008] , Hansen et al. [2010c]	MP
Colonoscopy Maps	Vos et al. [2003] , Paik et al. [2000]	MP
Aneurysm Maps	Neugebauer et al. [2009a]	MP

TABLE e14.1 Projection and reformation techniques discussed in this chapter. AU = Anatomical Unfolding, APR/P = Anatomical Planar Reformation and/or Projection, MP = Map Projection. We list a subset of the references.

- Map projection techniques are named after the methods used in cartography to represent the surface of a sphere, typically the earth, on a plane in order to create a map. We explicitly include techniques that map non-spherical objects to a plane.

[Table e14.1](#) shows the list of techniques that we have selected, along with their types and an example reference.

14.3 ANATOMICAL UNFOLDING

In this section, we discuss four essential examples of anatomical unfolding. We start with the Bull's eye plot, a kind of anatomical unfolding that is frequently used in clinical practice and go on with brain cortex and colon unfolding. Brain cortex unfolding is widely used in neurosciences, whereas colon unfolding

is motivated by the efficient search for polyps and early stages of colon cancer along the complex colon anatomy. Multiply branched vessel unfolding is used to investigate branching blood vessel structures for stenoses and other pathologies.

14.3.1 CARDIAC BULL'S EYE PLOTS

In the introduction, we have already discussed the cardiac Bull's Eye Plot [Cerqueira et al., 2002a], where parts of the muscle wall (myocardium) of the left ventricle of the heart are projected onto 17 standardized segments, arranged into concentric circles. This can also be seen as an unfolding of the conical heart wall geometry onto the plane, with the apex of the cone being the innermost of the concentric circles. The great strength of this layout is that it is instantly recognized and understood by cardiologists and other cardiac imaging professionals worldwide. Complex 3D information can be mapped onto the 17 segments, and users are instantly able to reconstruct mentally the 3D origin of the projected information without the need for any interaction.

Termeer et al. [2007] identified three issues with the standard BEP, namely that the segments had the risk of giving a quantized view of the data, that they were not able to show both the amount of scar and the distribution of scar at the same time and that the traditional BEP did not provide any anatomical information. In order to address these limitations, they introduced the volumetric BEP, or VBEP.

Figure e14.2 shows the principle behind the construction of the VBEP. It is similar to the BEP in that the conical shape of the ventricle is unfolded onto the plane. However, where the BEP accumulated data through a particular segment of the heart wall and projected the accumulation onto the relevant segment of the plot, TERMEER proposed volume rendering the full thickness of the heart wall. This resulted in a continuous, instead of segmented, representation of the data. Furthermore, the VBEP was enhanced with anatomical context in the form of the projected coronary arteries as well as two dots representing the locations where the right ventricle meets the left ventricle. Figure e14.3 shows a BEP and VBEP side-by-side.

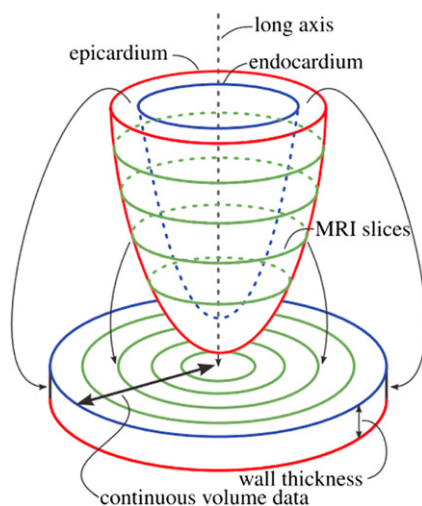


FIGURE e14.2 The principle behind the construction of the Volumetric Bull's Eye Plot (VBEP). The heart wall is unfolded in the same way as for the BEP, but the thickness of the wall is maintained through volume rendering. Furthermore, this results in a continuous, unsegmented visualization of information mapped throughout the thickness of the myocardium (From: [Termeer et al., 2007]).

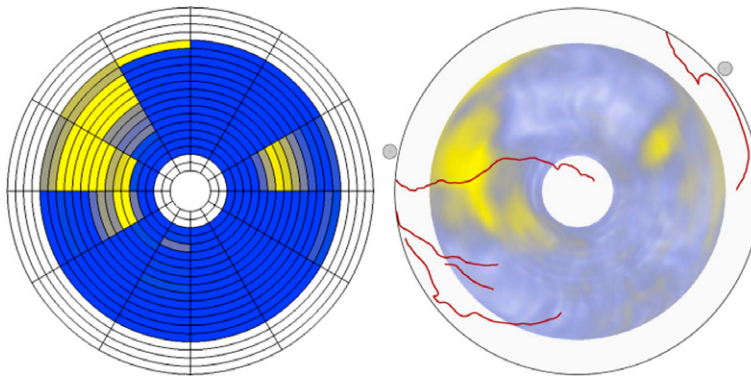


FIGURE e14.3 A BEP and VBEP side-by-side. The BEP aggregates and represents a single attribute value per segment, while the VBEP renders the underlying data continuously. The coronary arteries are projected as red lines, while the two dots outside the outermost circle show the locations where the right ventricle joins the left ventricle (From: [Termeer et al., 2007]).

14.3.2 BRAIN CORTEX FLATTENING

The outside layer of the brain is called the cerebral cortex. This layer consists of gray matter which is formed mostly by neurons. In humans, as well as in other large mammals, the cortex consists of many folds. It is estimated that between 60% and 70% of the cortex is buried in the grooves formed by the cortical folds, also known as the sulci [Zilles et al., 1988]. When analyzing or visualizing for example functional brain imaging data as acquired by fMRI, the folded nature of the cortex poses a challenge. How can neural activity, which takes place mostly in the folded cortex, be effectively visualized if such a large percentage of the cortex itself is hidden in folds?

In neuroimaging, this challenge is addressed with three different anatomical unfolding techniques [Fischl et al., 1999]:

- Inflation techniques “blow up” the cortical surface, thus smoothing out all folds.
- Flattening techniques make cuts in the surface in order to spread it out on a planar surface.
- Parameterizable surface mapping techniques map each point on the cortical surface to a different parameterizable surface, such as a sphere, so that different hemispheres can be easily compared.

Three examples are shown in Figure e14.4.

Although these three solutions had been explored before, Fischl et al. [1999] presented a unified method that minimizes metric distortion. Their iterative method employs different *cost functions* incorporating terms for maintaining the geodesic distances between cortical surface points and their neighbors (this minimizes the metric distortion), for removing folds in the surface by penalizing negative oriented face area, and for smoothing out the surface with a spring force. These methods are available in the **FreeSurfer** software,¹ a system widely used in the neuroimaging community. Ju et al. [2005] quantitatively evaluate and compare Fischl’s methods with five alternative approaches for cortical surface flattening.

¹ <http://surfer.nmr.mgh.harvard.edu/>.

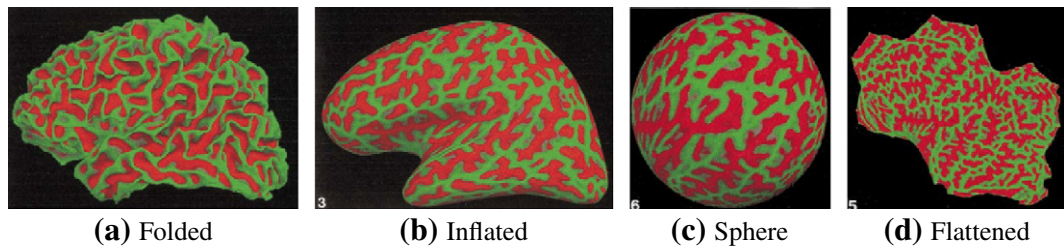


FIGURE e14.4 Three different ways of anatomically unfolding the brain cortex: inflation, mapping to a sphere and flattening (From: [Fischl et al., 1999]). Sulci are red and gyri green in all cases.

14.3.3 COLON UNFOLDING

In virtual colonoscopy (§ 13.6.1), graphics techniques are used to render the inside of the colon based on CT data, so that polyps, fleshy outgrowths on the inside wall of the colon that are precursors of colon cancer, can be visually detected. The colon also contains many folds, resulting in a significantly larger inner surface for the absorption of nutrients from food. However, inspecting the inside wall of the colon is complicated, as large parts of the surface, including potentially polyps, are hidden inside colonic folds. Colon unfolding techniques address this problem by attempting to flatten all folds, then to open up the tubular colon and finally to project the flattened and opened-up colon to a plane for inspection.

Early techniques to unfold the colon were straightforward [Wang and Vannier, 1995]. First, the centerline of the colonic cavity was computed. Then, a number of cross sections, orthogonal to the centerline and sampled over its length, were determined. The centerline was then straightened and the cross sections stacked upon each other accordingly. The straightened colon contained by the stacked cross sections was then unfolded and viewed using standard volume rendering techniques.

However, sharp curves in the centerline would cause cross section undersampling on their outsides and intersecting cross sections on their insides. This could lead to respectively missing polyps or rendering geometry multiple times. Therefore, several improvements have been proposed. In a follow-up publication addressing the intersection problem, Wang et al. [1998] suggested to use curved cross sections determined by simulated electrical field lines exiting from electrical charges distributed over the length of the colon centerline. When this is done with charges distributed over the full length, curved cross sections would not intersect, but the method could still cause substantial distortion due to oversampling and undersampling. This problem was alleviated by considering only a 2.5 cm window along the colon centerline around the currently extracted cross section. The technique was qualitatively evaluated by a radiologist, experienced in virtual colonoscopy, on two patient datasets.

Unfolding by Non-Linear Ray Sampling By casting rays initially radially outwards from the colon centerline for each successive cross section, but then following the gradient direction of the centerline distance map, Vilanova et al. [2001] efficiently solved the problem of intersecting cross sections. Figure e14.5 shows the difference between standard orthogonal cross sections and non-linear rays. The volume data was sampled along each curved ray and volume rendering was performed, stopping when the ray hit the colon wall. This resulted in a 2D parameterization of the inside colon wall, with the distance along the centerline being the one parameter and the radial index of the ray within its cross section being the other. The sampling of the colon wall by this parameterization was of course not uniform, so a direct mapping to 2D would result in severe distortions. The sampling was therefore nonlinearly scaled, using an iterative algorithm, to compensate for these distortions and maintain area preservation. Finally, undersampling in

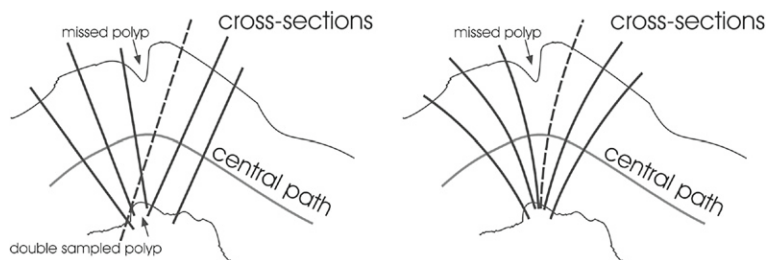


FIGURE e14.5 On the left, a 2D view of cross sections orthogonal to the colon centerline with a missed and doubly sampled polyp shown. On the right, non-linear ray sampling solves the multiply sampled geometry problem, but without undersampling correction could still miss polyps (From: [Vilanova et al., 2001]).



FIGURE e14.6 Unfolded colon after non-linear sampling (From: [Vilanova et al., 2001]).

the resultant scaled grid was detected and remedied by interpolating extra intermediate samples from the inside colon surface. This approach efficiently yields overviews of the complete inner surface of the colon, while minimizing distortion, duplication and undersampling. It was tested on three datasets, and in one case also compared with a physical dissection, but not yet clinically evaluated. Figure e14.6 shows an example of a colon that has been unfolded using this technique.

Unfolding by Conformal Mapping Haker et al. [2000] took a different approach to colon unfolding in basing their technique on an explicit triangulated surface representation of the colon, which could then be conformally mapped onto a flat surface. A *conformal mapping* preserves angles, and hence the local geometry of the folded colon surface. The method made use of a finite element procedure to approximate numerically the function mapping from the folded colon surface to the plane. It resulted in a completely flattened geometry which had to be visually enhanced either with a surface coloring representing mean curvature or a shading map (that is the mapped normals from the original unflattened surface) to facilitate surface feature recognition in the flattened view. This method was not evaluated for clinical use.

Hong et al. [2006] presented a related approach, in that they also started from a triangulated mesh which was then conformally mapped to the plane using the finite element method. However, their approach introduced two interesting variations. First, they employed an explicit step for the removal of small topological handles from the mesh, thus filtering out this type of topological noise.

Second, they used direct volume rendering (DVR) techniques (see § 7) to render the flattened colon image, in order to add shading and hence to improve shape perception of the embedded polyps in the flattened representation. For each pixel in the flattened image, the corresponding 3D position and camera

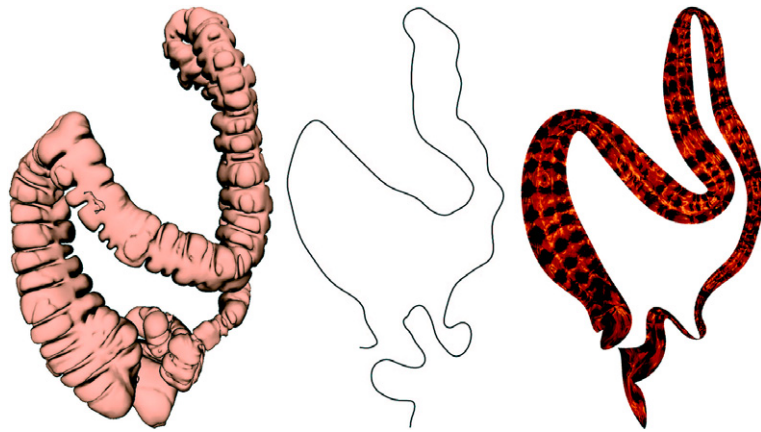


FIGURE e14.7 Context-preserving maps of tubular structures. On the left the original colon surface is shown. In the middle the 3D centerline has been mapped to 2D, and on the right the colon has been conformally mapped to the plane and deformed according to the 2D centerline (From: [Marino et al., 2011]).

would be used by a GPU fragment shader to calculate the correct shading. The work does not mention any clinical evaluation.

Up to now, all colon unfolding techniques also straightened the colon, yielding a single rectangular image. This facilitates finding polyps in a single view. However, the 3D trajectory of the colon is completely discarded in the process, leaving only the length along its centerline to help the user with localization. To address this problem, Marino et al. [2011] proposed deriving context-preserving maps of tubular structures, in which they unfolded the colon using the same harmonic mapping approach as Hong et al. [2006], but managed to project its 3D trajectory onto the plane while still retaining a large part of its 3D trajectory (see Fig. e14.7).

After deriving the centerline (or 3D skeleton) of the colon, it was projected either onto its best anatomical view plane, or, if that is not known, a plane that minimizes structural overlap and centerline intersections. After this initial projection step, the projected centerline segment length was corrected for projection distortion, after which intersections were removed and finally close segments were spaced apart.

The colon surface was then conformally mapped to the plane, after which that plane was deformed according to the projected centerline of the colon. This would yield a flattened map that still managed to retain a great deal of the context contained in the 3D trajectory of the colon. This context-preserving flattened map could then be rendered using volume rendering techniques, as explained previously.

Map projections have also been employed in the context of virtual colonoscopy. This is discussed in § 14.5.3.

14.3.4 MULTIPLY BRANCHED VESSEL UNFOLDING

In contrast to the colon, which has no branches, blood vessels often branch, forming trees with multiple branch points. The unfolding of these multiply branched structures is also possible, as was shown by Zhu et al. [2005]. They first showed how a Y-shaped vessel bifurcation could be conformally mapped to the plane. This was done by constructing three smooth curves, running from the base of the Y to the point at which it splits into two branches, and then up the two respective branches. These curves define a cut

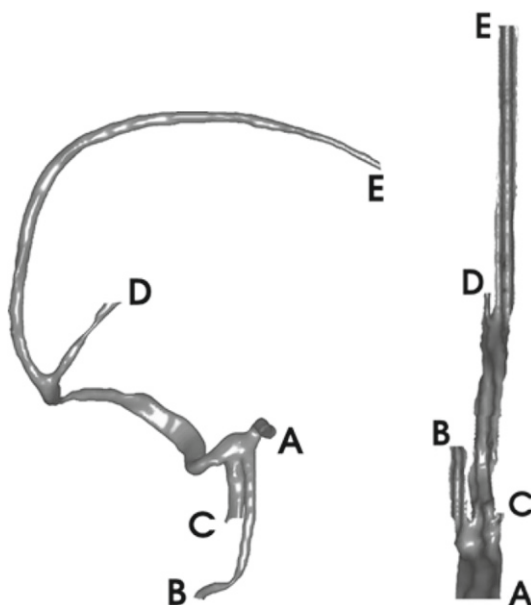


FIGURE e14.8 Conformal mapping of multiply branched vessels from brain MRA. On the left is the original surface, on the right the conformally mapped, non angle-preserving, map view. Vertices have been shaded with their original normal vectors (From: [Zhu et al., 2005]).

on the Y-shaped surface that could be used with the finite element method to determine a conformal mapping to the plane.

For conformally mapping a more complex multiply branched vessel tree, they would first determine the harmonic skeleton of the vessel tree. The *harmonic skeleton* is similar to the central line or straightforward skeleton, but was called so due to its particular implementation. A surface-based region growing was started at the root of the tree. Whenever a branch point was reached, the triangle-based distance from the root would be associated with it. By determining the centroids of clustered distance values, the central line could be determined. In subsequent steps, the skeleton was refined.

With this skeleton, the vessel tree could be decomposed into multiple Y-shaped segments, each of which could be conformally mapped to the plane. This would finally yield a single view of the whole tree on the plane, that could optionally be further processed to yield also an area-preserving mapping. Figure e14.8 shows an example of applying this approach to a brain MRA dataset. Curved planar reformation, see § 11.3.3, offers a different method, one that does not employ explicit unfolding or conformal mapping, for the visualization of curved and branching structures on the plane.

14.4 ANATOMICAL PLANAR REFORMATION/PROJECTION

As mentioned above, anatomical planar reformation and projection techniques derive a planar geometry based on the most relevant anatomical structures for a given problem domain, then reformat or project the original data along or onto that geometry, finally flattening the planar geometry along with the data. One of the most well-known examples of anatomical planar reformation techniques is CPR

[Kanitsar et al., 2002, Vrtovec et al., 2005], where the planar geometry is formulated along vascular structures that are to be visualized, which finally results in a 2D flattened visualization of the vascular structures and their surroundings. CPR is discussed in some detail in § 11.3.3 where also branching multivessels are considered. In this section, we will examine two additional examples, one based on projection and the other on reformation. In both cases, elongated tubular structures are involved. The techniques are motivated by the diagnostic goal of detecting any suspicious change along the tubular anatomy.

14.4.1 TUBULAR STRAIGHTENING

Angelesli and Hauser [2011] presented an anatomical planar projection approach for visualizing flows through tubular structures, applied to the specific problem of visualizing blood flow through the human aorta as measured with Phase-Contrast MRI (PC-MRI). Their technique is based on determining the centerline of the aorta and then either reformatting the original space and data, or reformatting flow visualization primitives, along the straightened centerline. In the former case, the straightened data domain can be visualized with traditional flow visualization techniques.

Tubular straightening offers similar advantages to other planar reformation techniques: The focus structure, for example the aorta, along with the information in and around it, has been straightened so that it can be more easily viewed in its flattened configuration. Also due to the same structure being flattened in the same way, side-by-side comparisons become more useful. Figure e14.9 shows the general procedure behind tubular straightening and side-by-side comparison.

Rib Straightening Kiraly et al. [2006] presented a similar technique for the visualization of ribs from CT data. Such rib visualizations are primarily motivated by the search for bone metastasis in the case of cancer patients. In conventional slice-based or 3D visualizations, the mandatory search for such metastasis

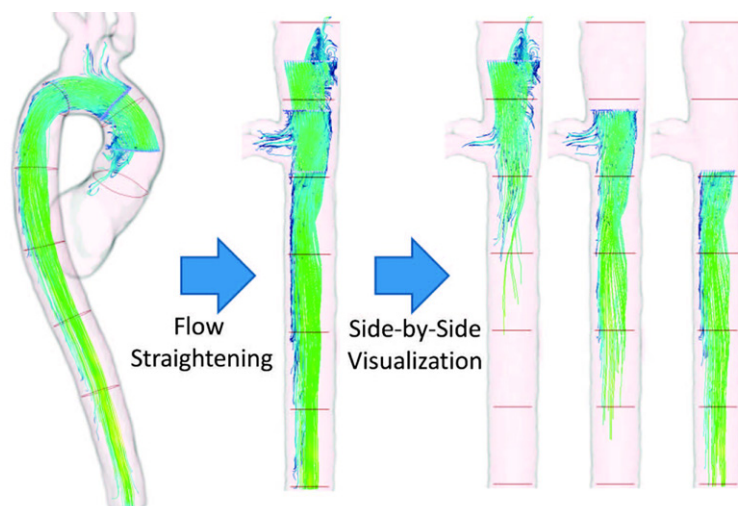


FIGURE e14.9 Straightened aorta with streamlines visualizing the blood flow for a single timestep. Due to the straightening, different timesteps or, in this case, different streamline seeding configurations can be shown side-by-side (From: [Angelesli and Hauser, 2011]).

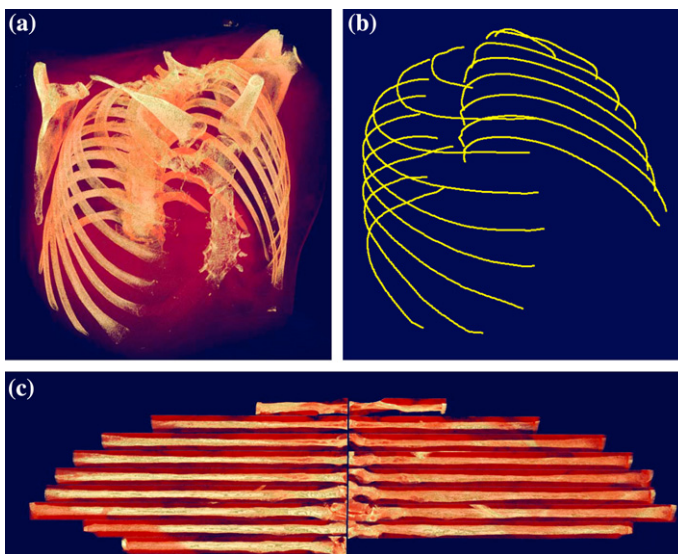


FIGURE e14.10 Example of the rib straightening technique. At the top left, a volume rendering of the original CT data. At the top right, the extracted and smoothed centerlines. At the bottom, a single slice through the straightened data (From: [Kiraly et al., 2006]).

is tedious. After segmenting the ribs and determining their smooth centerlines, the data around each rib was reformatted by resampling from planes positioned orthogonally to its centerline, at regular intervals along its length. The straightened volumes for each rib were then combined into a single dataset which could be visualized using any of the standard 3D visualization techniques. The authors found that simply viewing the slice cutting through the centers of all ribs yielded the best results. This view enabled the simultaneous investigation of all ribs, for example for tumors, where traditional 3D visualization of the non-straightened dataset would require a great number of interaction steps. Figure e14.10 shows an example of the rib straightening procedure.

Evaluation The aorta straightening technique was evaluated informally with the cardiovascular MRI group at an academic hospital [Angeles and Hauser, 2011]. The group believed the reformatting to be potentially useful for comparison of flow parameters in a research setting, but for clinical staff it would require some training, as physicians were used to seeing the blood flow in its original context. The authors make the good point that CPR initially also required training but has since then been embraced by clinical practitioners.

14.4.2 ARTICULATED PLANAR REFORMATION

In molecular imaging research experiments, groups of small animals are imaged with different modalities at different time points. In general, animal movement can't be constrained, so postures are potentially different for each animal, at each timepoint and for each modality. This greatly complicates high-level and fine-grained comparison between different animals and between timesteps, a central activity in molecular imaging research.

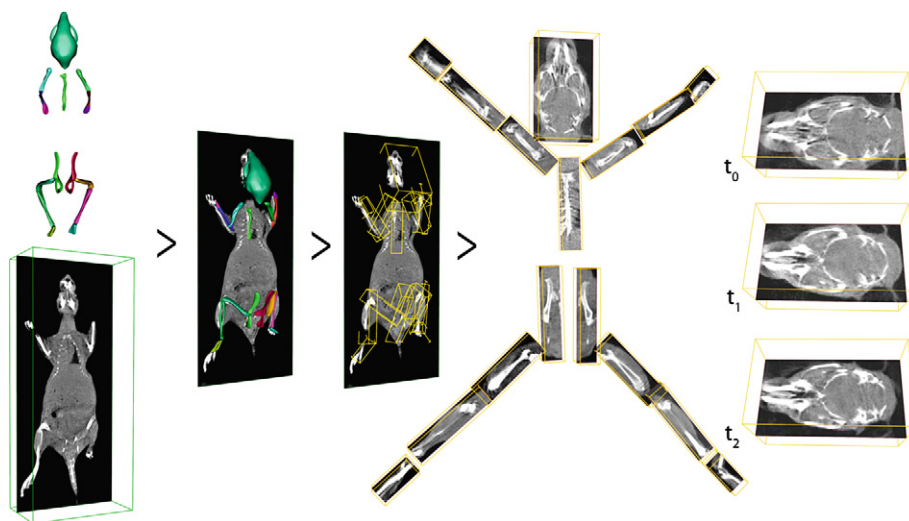


FIGURE e14.11 The complete articulated planar reformation (APR) processing pipeline [Kok et al., 2010]. First, a labeled skeletal atlas is mapped to the new data using articulated registration. Using the known location of all atlas bones in the new data, sub-volumes surrounding these bones are calculated using PCA. These sub-volumes are transformed back to a standardized flattened skeleton space where different datasets can be easily compared (Courtesy of Peter Kok, Delft University of Technology).

Kok et al. [2010] addressed this problem by reformatting the data based on a standardized planar (flattened) arrangement of a mouse atlas skeleton, and then visualizing the original data reformatted along this flattened skeleton. Figure e14.11 shows all steps of the presented procedure.

All small animal datasets were mapped to the same mouse atlas skeleton via articulated registration [Baiker et al., 2010]. In articulated registration, the mouse atlas skeleton is registered fully automatically to any CT dataset by taking into account the different range of motion constraints of each skeletal joint. Using the iterative closest point transform, the different bones are registered in a hierarchical fashion to the CT data: First the spine, then the head taking into account the neck range of motion, then the upper arms taking into account the range of motion of the shoulders, and so forth.

As a result of this registration, each of the bones in the mouse atlas skeleton could be positioned in the target CT dataset. Using principal component analysis, object-aligned bounding boxes surrounding each of the bones in the CT dataset could be determined. These bounding boxes, along with the CT data that they contained, were then mapped back to the planar layout of the mouse atlas skeleton.

This process was repeated for all mice and all timepoints, after which global and local comparisons could be more easily performed. For global comparison, difference metrics could be mapped onto the mouse atlas skeleton, while for local comparison the user could zoom in on any of the now planar bones and perform side-by-side comparisons of the raw CT data.

Evaluation The technique was evaluated separately with the scientific leaders of two large small animal and molecular imaging research groups, who found the standardized planar layout to be a valuable tool for comparison of study data. The possibility of performing group studies, that is being able to reformat the data of a large cohort of small animals, could be of significant added value.

14.5 MAP PROJECTIONS

Map projection techniques usually refer to techniques that map from the sphere to the plane. Here we additionally discuss techniques that map from other 3D shapes to the 2D plane. We begin with tumor maps, an anatomical structure usually with a roughly spherical shape.

14.5.1 TUMOR MAPS

Percutaneous radio-frequency (RF) ablation is a minimally-invasive therapy that can be used to treat tumors in the liver. Electrodes are inserted via needle-puncture of the skin and used to heat up and kill tumor cells. Pre- and post-treatment CT scans are used to evaluate the effectivity of the treatment by checking that tissue has been coagulated everywhere within the tumor and in a safety margin surrounding it.

Rieder *et al.* [2010] introduced tumor maps to facilitate this evaluation. By calculating the intersection of the segmented tumor with the coagulation volume and its safety margin, tumor tissue can be classified into three parts: tumor tissue that lies inside the coagulation safety margin is assumed to have undergone complete cell destruction (shown in green), tumor tissue that lies within the coagulation region but outside the safety margin has probably undergone cell destruction, but there is some risk that this is not the case (shown in yellow) and tumor tissue that falls completely outside of the coagulation region has not been successfully ablated (shown in red).

As shown in Figure e14.12, the color-coded tumor surface is shown in its 3D context, and visualized with a tumor map which shows the complete color-mapped outer surface of the tumor map projected onto the 2D plane, in this case using the area-preserving Mollweide map projection. By default, the authors employ a longitude-latitude mapping, a cylindrical mapping that simply maps longitude and latitude to a rectangular coordinate system. Due to the distortion at the poles, they then optionally apply either the area-preserving sinusoidal projection or the area-preserving Mollweide projection. The tumor map is further enhanced with directional cues, being primarily the A, P, L, R, H, and F (anterior, posterior, left, right, head, foot) labels, well-known from medical imaging workstation consoles.

Using the tumor map, the full outside surface of the tumor, color-coded with the three different coagulation zones, can be viewed in a single 2D image. However, the anatomical context is missing. To address this issue, the authors designed synchronized interaction between the tumor map and the

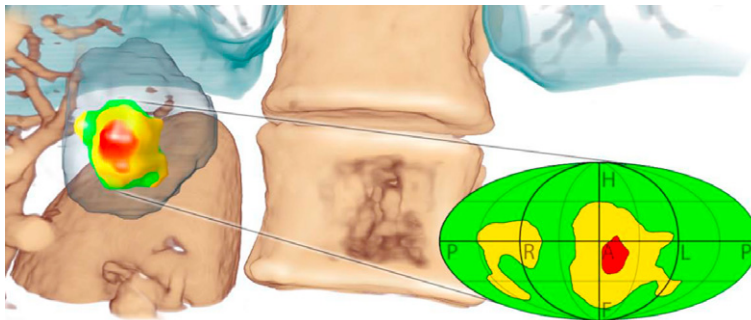


FIGURE e14.12 A visualization of the tumor in its 3D context, with the traffic light color scheme used to represent ablation state. The inset shows the 2D tumor map, which is a pseudo-cylindrical mapping of the tumor surface with labels for head, foot, left, right, anterior and posterior to facilitate orientation (Courtesy of Christian Rieder, Fraunhofer MEVIS. See also [Rieder *et al.*, 2010]).

accompanying 3D visualization. Clicking on the tumor map highlights the corresponding point in 3D, while dragging on the tumor map rotates the 3D view accordingly.

Evaluation The authors made the case that the advantage of being able to view the entire outside surface of the tumor was obvious enough not to require an evaluation. Instead, they evaluated in a user study with fifteen users whether scene rotation to pre-specified zones of interest via the tumor map was faster than traditional methods, and found that navigation with the straightforward longitude-latitude map was the fastest, followed by the Mollweide, and that both were significantly faster than normal trackball rotation. An informal evaluation was also conducted with five experienced physicians, who found the tumor map useful for the initial observation of ablation zones, and for the initial marking of suspicious areas.

14.5.2 LIVER RESECTION SURFACE MAPS

Liver tumors are surgically removed in a process called hepatectomy, or liver resection. During this procedure the part of the liver containing the tumor is surgically removed, avoiding as far as possible critical structures such as the portal and hepatic veins. During the surgical planning stage, a straight or curved resection plane, along which the liver will be resected, is specified. This is explained in more detail in [Section 17.5.4 of Chapter 17](#).

[Lamata et al. \[2008\]](#) first proposed using a simplified representation of the planned Resection Map and critical structures for intraoperative visualization, and called their representation the *Resection Map*. The Resection Map consisted of two views. The surgical view showed the resection plane orthogonal to the view plane, along with risk structures within a user-configurable distance to that plane and within the *progress window*. The progress window was defined on the second view, called the progress view, showing the resection plane parallel to the view plane. In this view, all critical structures could also be seen, with color-coding to represent their closeness to the resection plane. [Figure e14.13](#) shows an example of the Resection Map display.

[Hansen et al. \[2010c\]](#) extended this idea by projecting critical structures (tumor, hepatic and portal veins) onto the resection surface. The distance of the critical structures to the resection surface was also represented by a segmented color-coding as can be seen in [Figure e14.14](#).

Evaluation Based on a preliminary and informal evaluation by surgeons, Risk Maps “may prevent a possible damage to risk structures and thus enhance patient safety during liver surgery” [[Hansen et al., 2010c](#)]. In follow-up work, Risk Maps were further evaluated in two studies measuring whether and how Risk Maps facilitate the process of surgical risk assessment [[Hansen, 2012](#)]. In the first study, resection planes were presented to three experienced surgeons, randomly with or without Risk Maps, after which they had to mark areas at which they expected risk or difficulty during the resection. Surgeons were faster with Risk Maps, but not significantly so. Through the accompanying questionnaire they did indicate that Risk Maps were helpful in assessing risk. In the second experiment, a mix of scientists and radiological technicians had to identify risk structures close to a virtual instrument tip, with and without using Risk Maps. Identification of risk structures was significantly faster with Risk Maps than without.

Resection Maps were first evaluated with guided interviews with five surgeons from two European hospitals [[Lamata et al., 2008](#)]. During these interviews, surgeons indicated that the risk maps could potentially lead to an increase in confidence and that they could serve as a sufficient guidance tool. Resection Maps would have the most utility supporting irregular resection planes. Surgeons would have preferred the progress window to update automatically. In a follow-up study, the technique was further evaluated with three surgeons from three hospitals using Resection Maps in the execution of seven hepatectomies [[Lamata et al., 2010](#)]. Based on the Likert scale questionnaire, Resection Maps were positively received.

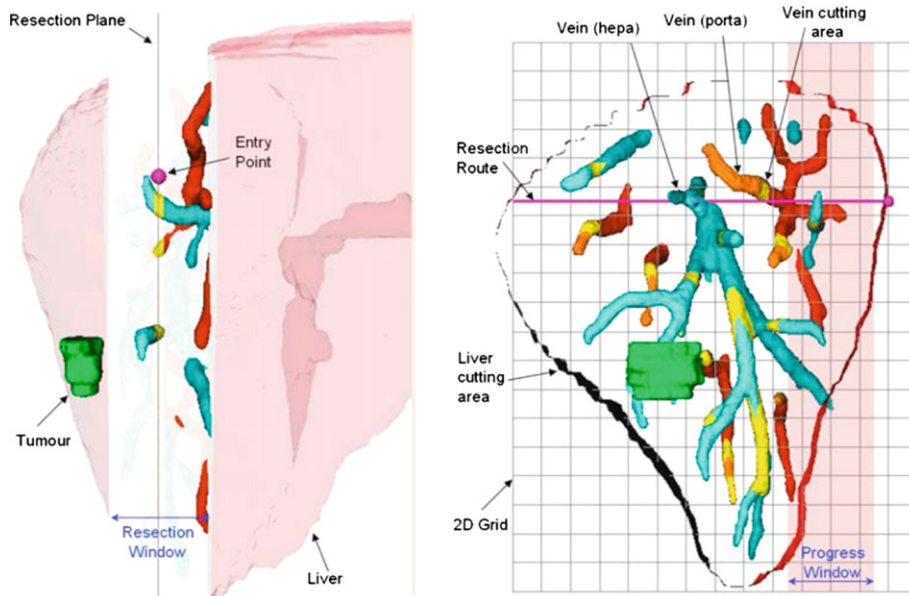


FIGURE e14.13 The Resection Map as proposed by Lamata et al. [2008]. On the left the surgical view is shown, and on the right the progress view.

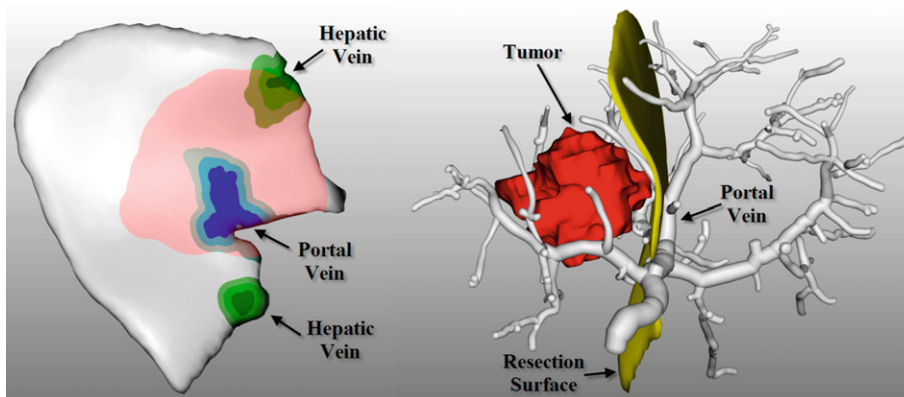


FIGURE e14.14 On the left, an example of the liver risk map, showing the proximity of the tumor in red, and the hepatic and portal veins in green and blue, respectively. The distance of the hepatic and portal veins is encoded in lighter color segments. On the right, the curved resection plane is shown in its anatomical context (From: [Hansen et al., 2010c]).

14.5.3 COLONOSCOPY MAPS

In Section 14.3.3, anatomical unfolding was employed to flatten the folds and virtually dissect the colon, resulting in a flattened surface that can in principal be inspected more easily for polyps.

Paik et al. [2000] investigated Mercator and stereographic map projections as an alternative solution to the problem of ensuring visibility of a large percentage of the folded colon wall. Instead of unfolding

and dissecting the colon, flythroughs are generated along the colon centerline. At regular points along the centerline, a map projection of the full surroundings was generated, instead of just the forward and backward facing views, as was commonly done. The map projection results in a flattened view of the full surrounding colonic landscape. This is the same as a map projection of the earth, except that the observer finds itself within the colon looking outward.

This theme was further explored in [Serlie et al. \[2001\]](#), where the authors proposed rendering six projections at 90° viewing angles at regular points along the centerline, and then displaying flythroughs as a sequence of unfolded cubes.

Evaluation On nine random patient datasets, it was found that the Mercator map projection guaranteed 98.8% surface visibility. Forward and backward facing views could only compete with this at a high view frustum angle, which resulted in quite some visual distortion and hence lower sensitivity. With two experienced radiologists and synthetic polyps in a real dataset, more polyps were detected with Mercator and stereographic map projects than with normal endoscopic rendering or even viewing raw axial slices.

The unfolded cube technique was compared with forward and backward facing views [[Vos et al., 2003](#)]. Two experienced radiologists used both display methods to study the data of thirty patients. It was found that the unfolded cube was significantly faster and ensured more visibility of the inner colon surface, although sensitivity and specificity were not significantly different between the two methods.

14.5.4 ANEURYSM MAPS

Blood flow simulations result in flow data and scalar flow features, such as pressure, velocity, and wall shear stress (WSS). In particular, WSS plays an essential role in the understanding of initiation and progression of vascular diseases. A simple solution to display scalar flow features is to show the surface of the relevant vascular region with the scalar flow feature color-mapped onto it.

The disadvantage of this simple solution is that only a small portion of the surface is visible at the same time. By using a map projection that shows the five sides not currently facing forward, in a flattened arrangement, all scalar information can be shown simultaneously. However, a map exhibits distortions. Furthermore, a simple map can be hard to relate to the complex 3D anatomy of pathological vessels. A combination of a faithful 3D anatomy representation and a map view, where interaction in both views are synchronized, could help to address this problem.

[Neugebauer et al. \[2009a\]](#) introduced a map display for scalar flow features where the 3D anatomy model is presented in a central part and flow features of the left, right, bottom, up, and back side are presented as flat regions of a map surrounding the anatomical view. When the user selects a point in one of the map views and drags it toward the center, the 3D anatomy model is rotated such that this point becomes visible (see [Fig. e14.15](#)). Also, a rotation of the 3D view of the anatomical model is possible and results in an update of the map views. This enables a systematic exploration of all regions. Neuroradiologists emphasized that this technique enables a better exploration of scalar flow features at opposite sites. There are many details to consider, such as map layout, interaction techniques, color selection and display of additional hints that are discussed in [Neugebauer et al. \[2009a\]](#).

Despite encouraging feedback so far, more evaluation and corresponding refinements are necessary to make this strategy broadly applicable. While it is applicable to non-stationary flows in principle, it is likely that modifications are necessary if the scalar flow features change over time and lead to frequent changes of the map view and the 3D model view.

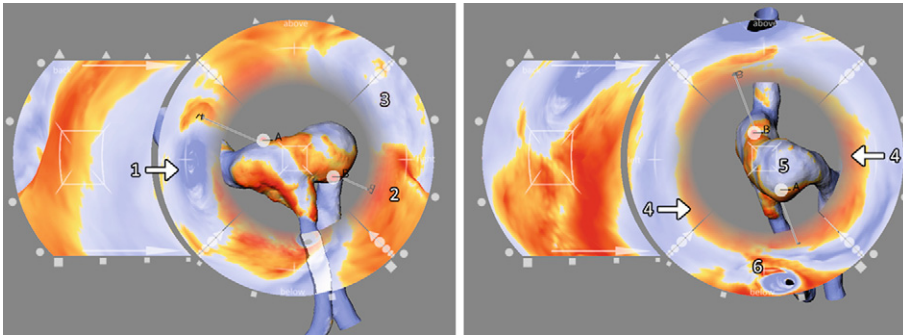


FIGURE e14.15 A 3D model of the relevant vascular anatomy is surrounded by map views that display scalar flow features of five sides (features at the left, right, bottom, and up side are shown at the corresponding ring portions). Scalar features of the backside are shown at the most right display. The lines pointing from the map portions to the 3D view indicate correspondences, where scalar features are shown in both views. If the user drags a point, representing an interesting feature from a map view to the center, the anatomical model is rotated to make that region visible. All map views change accordingly (From: [Neugebauer et al., 2009a]).

14.6 CONCLUSION

In this chapter we have discussed a number of medical visualization techniques that deal with the problem of intelligently transforming 3D data into 2D. The techniques are based either on reformation or projection. Reformation-based techniques sample data along a certain geometry embedded within the source 3D dataset, and then flatten that embedded geometry, taking the sampled data with it. Projection-based techniques aggregate data over any number of arbitrarily defined projection frustums.

We further grouped the techniques into three types. Anatomical unfolding techniques make use of an anatomically defined, usually folded, surface in the data, which is then unfolded and flattened, along with the data defined on or close to it. Anatomical planar reformation and projection techniques define a planar geometry, guided by tubular or skeletal structures in the data, and then flatten the planar geometry, along with the data defined on or close to it. Map projection techniques, originating from cartography, employ various approaches to project 360° views to 2D. The choice of technique type is guided by domain expertise and tasks on the one hand, and by what can be extracted from the data on the other. For example in the case of CPR, the domain task is to inspect visually the condition of a geometrically complex blood vessel, focusing on abnormalities such as stenoses, occlusions, aneurysms, and vessel wall calcifications. Furthermore, the blood vessel can be extracted from the data. Because the blood vessel geometry is available, and a plane intersecting the vessel is appropriate for detecting the mentioned abnormalities, a planar reformation is the most suitable technique type.

Ware [2001] argued that, based on the characteristics of human spatial perception, we should definitely favor 2D layout over 3D when designing graphics. Furthermore, he recommended that 3D objects should be used to represent data entities, in the context of a 2D layout, as such objects are easier to identify and remember. The techniques discussed in this chapter satisfy these, and to a certain extent all the other, guidelines that form part of Ware's $2\frac{1}{2}$ -D attitude to the design of visual displays. Through intelligent projection or reformation, three-dimensional medical data is transformed to a two-dimensional layout, while maintaining the three-dimensional characteristics of embedded objects. These representations offer advantages in terms of minimizing occlusion and in terms of enabling effective interaction, for example the fast rotation-to-target demonstrated by Rieder et al. [2010].

Based on the perceptual and interaction advantages, together with the observation that medical datasets are steadily growing in size and complexity, we think that projections and reformations that are able to simplify 3D to 2D in an elegant and effective fashion will become increasingly important and widespread in medical visualization.